

Assessing a BN-Doped Graphene for the Drug Delivery of Hydroxyurea Anticancer

Kun Harismah ¹ , Dinesh Kumar Sain ² , Mohammed Fanokh Al-Owaidi ³ , Hasan Zandi ^{4,*} ,
Atipan Saimmai ⁵ 

¹ Department of Chemical Engineering, Faculty of Engineering, Universitas Muhammadiyah Surakarta, Surakarta, Indonesia; kun.harismah@ums.ac.id (K.H.);

² Department of Chemistry, Faculty of Science, S.P. College Sirohi, Sirohi-307001, Rajasthan, India; frannydippu@gmail.com (D.K.S.);

³ Pharmaceutical Chemistry Department, College of Pharmacy, University of Kerbala, Kerala, Iraq; mohammed.f@uokerbala.edu.iq (M.F.A.O.);

⁴ Department of Chemistry, Faculty of Science, University of Qom, Qom, Iran; h.zandi.dr@gmail.com (H.Z.);

⁵ Faculty of Agricultural Technology, Phuket Rajabhat University, Muang, Phuket 83000, Thailand; atipan.s@pkru.ac.th (A.S.);

* Correspondence: h.zandi.dr@gmail.com (H.Z.);

Scopus Author ID 14122606900

Received: 10.09.2022; Accepted: 9.10.2022; Published: 6.01.2023

Abstract: A boron-nitrogen (BN)-doped graphene (G) was assessed in this work for approaching the drug delivery of hydroxyurea (HU) anticancer. Density functional theory (DFT) calculations were performed to optimize the structures and evaluate their related features. The results showed a possibility of the formation of four HUG bimolecule models during the optimization calculations. Further analyses of the modes indicated the existence of physical interactions between HU and G substances with meaningful levels of strength. Additionally, the models were analyzed regarding their molecular orbitals features, and the results indicated a possibility of conducting a measurement process to recognize the formation of the bimolecule model and its type of relaxation. Based on such obtained molecular orbitals features, a protective role of the G surface for the adsorbed HU was observed for preventing it not to participate in other interactions/reactions for approaching a targeted drug delivery process. The HUG models were observed with the major localization of molecular orbitals at the surface of the G structure. Indeed, all four obtained bimolecule models were suitable for forming HUG models by adsorbing the HU substance at the G surface with a deterministic role of the BN-doped region for managing the involved interactions. As a final remark, the results showed a possibility of employing the G surface for approaching the drug delivery platform of HU anticancer.

Keywords: graphene; hydroxyurea; adsorption; cancer; DFT.

© 2023 by the authors. This article is an open-access article distributed under the terms and conditions of the Creative Commons Attribution (CC BY) license (<https://creativecommons.org/licenses/by/4.0/>).

1. Introduction

Graphene has been found as a wonderful model of nanostructures after the pioneering innovation of carbon nanotubes [1-4]. The graphene's honey-comb layer-like architecture made it a very suitable surface for adsorbing other substances in atomic and molecular forms [5-8]. In this regard, several attempts have been dedicated to learning the details of such interacting systems to develop new functions of nanostructures for approaching drug delivery purposes [9-12]. It is known that the features of nanostructures made them distinguished materials for working with high efficiency on small scales [13-16]. Accordingly, several attempts have been

made to enhance the nanostructures for specific purposes, especially in biologically related systems [17-20]. Compositions of materials and nanostructures are important for showing characteristic structural and electronic features [21-24]. In this regard, modifying nanostructures could make them more specific for working in the desired functions. They have been seen as useful in adsorbents or sensor and biosensor devices [25-28]. A nanostructure could be modified by adding some atoms or functional molecular groups [29-32]. In terms of atomic modifications, some atoms of the original nanostructure could be replaced by other atoms to yield doped atomic models [33-36].

In most cases, the new doped nanostructure region could work as an active site of interactions to participate directly in interactions or induce neighborhood atoms' tendency to participate in interactions [37-40]. Consequently, the atomic doped nanostructure could manage the interactions, especially for the modified homoatomic carbon nanostructures, in which the atomic dopants create a partial heteroatomic region for the [41-44]. In the current research work, two carbon atoms of a model of graphene were doped by one boron and one nitrogen atom to bring BN-doped graphene (G of Figure 1). It should be mentioned that the BN-doped region's existence could increase the graphene surface's ionic state for better participation in interactions [45-48]. Accordingly, the surface was provided for adsorbing the hydroxyurea (HU) anticancer for approaching the initial steps of drug delivery platforms by introducing a representative adsorbent for the carrier role by forming HUG complexes.

The field of developing anticancer agents is very important because of cancer's serious negative impacts on patients' health quality [49-52]. Besides the existence of varieties of anticancer agents, low efficiencies and high adverse effects are the main restricting factors for approaching a successful medication [53-56]. Accordingly, several efforts have been made to enhance the efficiency of anticancer up to now [57-60]. However, further investigations are still required on the topics of anticancer developments and dealing with cancer-related issues [61-64]. Indeed, due to the appearance of new diseases or the resistance to conventional treatments, exploring new medical treatment protocols is essential for caring for the human health system [65-68]. For many years, hydroxyurea (HU) has been used to treat chronic myelogenous leukemia and head and neck cancers [69-72]. HU is an antimetabolite with the major role of inhibiting cancer cell growth in the body [73-76]. Besides the benefits of medications by HU, rising adverse effects for the patients limit the applicability of this anticancer for the regular treatment of cancer [77-80]. Therefore, an enhancement of HU is needed to approach a better level of medication for cancer patients. To this aim, representative BN-doped graphene (G) was assessed in this work for the drug delivery of HU through formations of HUG complexes (Figure 1). Quantum chemical calculations were performed to obtain the optimized structures and their features regarding the benefits of employing computational tools for exploring complicated systems [81-84]. All obtained results were summarized in Tables 1 and 2 and Figures 1-3 to discuss this work's goal.

2. Materials and Methods

The models of this work were single molecules of HU and G and their HUG complexes in four relaxation configurations; HUG1, HUG2, HUG3, and HUG4 (Figure 1). The single models, including HU and G, were optimized first, and their combinations were re-optimized next to obtain interacting bimolecular of HUG complexes. For obtaining the biomolecules, all possible configurations of HU towards the G surface were examined, in which four HUG structures were finally converged by optimization calculations. The B3LYP-D3/6-31G* level

of density functional theory (DFT) was employed to perform calculations using the Gaussian program [85]. The models were stabilized, and their features, including relaxed geometries, interactions, and descriptors, were evaluated in terms of visual and numeric descriptions. The relaxed geometries and involving interactions are exhibited in Figure 1. Distribution patterns of the highest occupied and the lowest unoccupied molecular orbitals (HOMO and LUMO) were exhibited in Figure 2. Diagrams of the density of states (DOS) are illustrated in Figure 3. Additionally, the obtained results of the quantum theory of atoms in molecules (QTAIM) and interactions details were summarized in Table 1, and other molecular orbital-based energy descriptors were summarized in Table 2. As a consequence, the required results of this work were prepared to assess the benefits of employing BN-doped graphene (G) for the drug delivery of hydroxyurea (HU) anticancer by formations of biomolecules of HUG complexes.

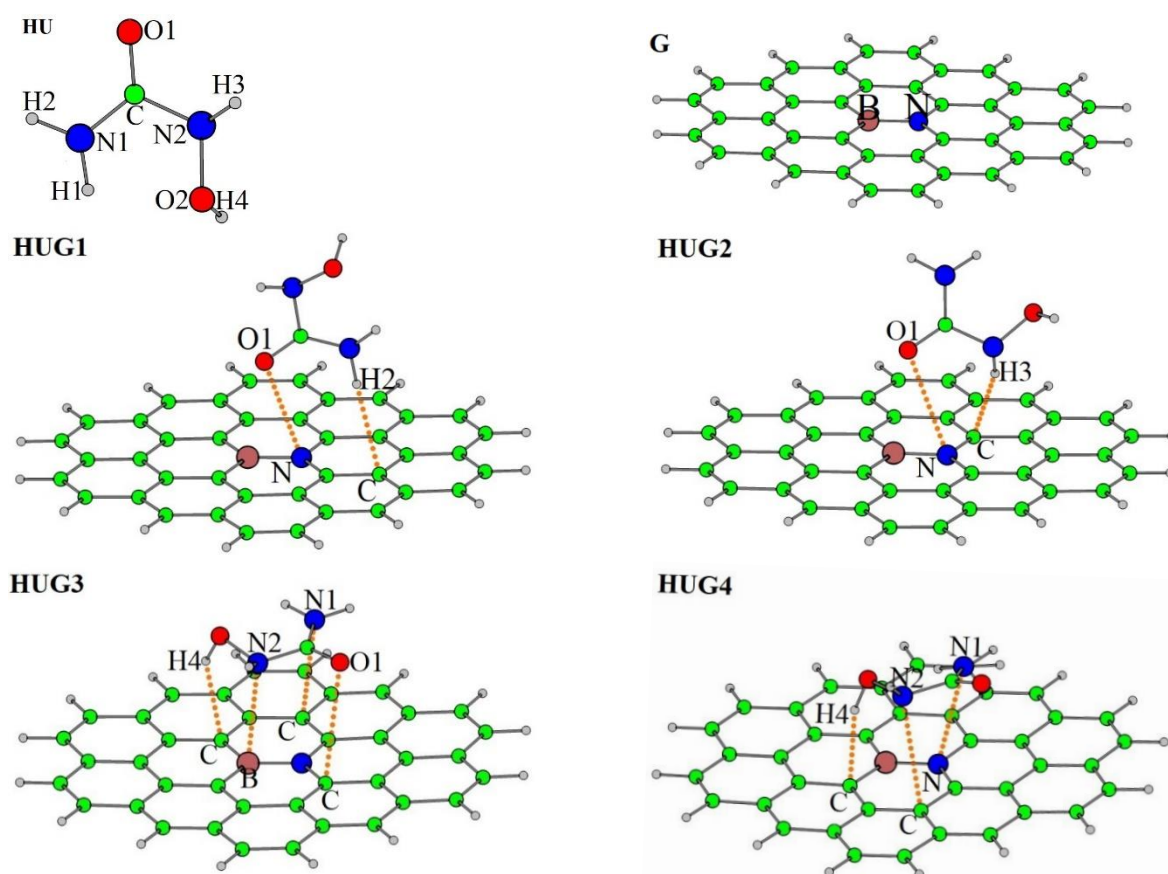


Figure 1. Optimized structures of single and bimolecule models.

Table 1. QTAIM and interactions features of HUG models.*

HUG Model	Interaction	Distance Å	ρ au	$\nabla^2\rho$ au	H au	ADS kcal/mol
HUG1	O1...N	3.084	0.0969	0.0305	-0.0569	-34.316
	H2...C	2.489	0.0103	0.0369	-0.0153	
HUG2	O1...N	3.191	0.0874	0.0267	-0.0501	-30.534
	H3...C	2.435	0.0113	0.0416	-0.0174	
HUG3	O1...C	3.294	0.0533	0.0203	-0.0852	-56.066
	N1...C	3.247	0.0803	0.0233	-0.0629	
	N2...B	2.917	0.0129	0.0324	-0.0489	
	H4...C	2.383	0.0127	0.0414	-0.0124	
HUG4	N1...N	3.157	0.0881	0.0293	-0.0811	-52.919
	N2...C	3.281	0.0739	0.0215	-0.0629	
	H4...C	2.289	0.0154	0.0465	-0.0957	

*The models are shown in Figure 1. The features of ρ , $\nabla^2\rho$, H, and ADS are bonding total electron density, bonding Laplacian of electron density, bonding energy density, and molecular adsorption energy.

3. Results and Discussion

The major goal of this work was to assess representative BN-doped graphene (G) for the drug delivery of hydroxyurea (HU) anticancer. To this aim, DET calculations were performed to optimize the geometries of the single HU and G models for preparing them to participate in HUG bimolecule complex formations. The optimization calculations yielded the minimized energy structures in both single and bimolecule states, as shown in Figure 1. Four models of complexes, including HUG1, HUG2, HUG3, and HUG4 were obtained by examining the possibilities of interactions between HU and G. Accordingly, the details of their interactions were analyzed using the QTAIM features [86]. As described in Table 1 for the exhibited interactions of Figure 1, the bonds of models were analyzed to show their features. Two interactions were involved in the formation of each of HUG1 and HUG2, four were involved in the formation of HUG3, and three were involved in the formation of HUG4. By examining the obtained results, HUG3 was placed at the highest level of interaction strengths among the four bimolecule models. Details of QTAIM features indicated what happened inside the molecular systems by showing the features of each bonding between the atoms of two molecules. Examining other results indicated the next levels of strengths for HUG3 > HUG1 > HUG2. The obtained values of molecular adsorption energy (ADS) indicated the orders of strengths of adsorptions or interactions between two molecules of HU and G. It could be mentioned here that formations of HUG bimolecule models were achievable, and details of interactions indicated the existence of physical adsorption for the models. Referring to the major goal of this work, HUG complexes could be obtained through the formation of physically interacting systems, and their stabilities were strong enough to propose the employed G structure as a possible carrier of HU. The BN-doped region's role was indeed in managing the occurrence of interactions, in which the HU substance was relaxed around the BN-doped region of the G surface. All four HUG bimolecular models were attached to each other with non-covalent physical interactions with reasonable strengths of interactions to yield strong, complex formations. Such physically interacting complexes are useful for conducting reversible adsorptions, in which the adsorbed substance could be able to be released by supplying the required energy of breaking involved interactions. Comparing the current results with other parallel works [87, 88] could show the benefits of employing HUG models for the drug delivery purposes of HU anticancer in a reversible but strong mode of interactions.

Table 2. Molecular orbitals energy features for single and bimolecule models.*

Model	EH	EL	EG	CH	CP	EI
HU	-6.964	0.962	7.925	3.963	-3.001	1.136
G	-4.853	-2.139	2.714	1.357	-3.496	4.503
HUG1	-4.763	-2.011	2.752	1.376	-3.387	4.168
HUG2	-4.761	-2.006	2.755	1.378	-3.384	4.155
HUG3	-4.804	-2.156	2.647	1.324	-3.481	4.574
HUG4	-4.974	-2.295	2.679	1.339	-3.635	4.931

*The models are shown in Figure 1. EH, EL, EG, CH, CP, and EI are all in eV as energy of HOMO, energy of LUMO, energy gap, chemical hardness, chemical potential, and electrophilicity index.

For determining the electronic features of investigated models, molecular orbitals energy features were evaluated for single and bimolecule states of the models (Table 2). HOMO implies the highest occupied molecular orbital, and LUMO implies the lowest unoccupied molecular orbital, in which their energies dominate, defining several other electronic features as could be seen by the obtained results, the values of EH and EL, implying

that the energy levels of HOMO and LUMO, were changed from the single to bimolecule states.

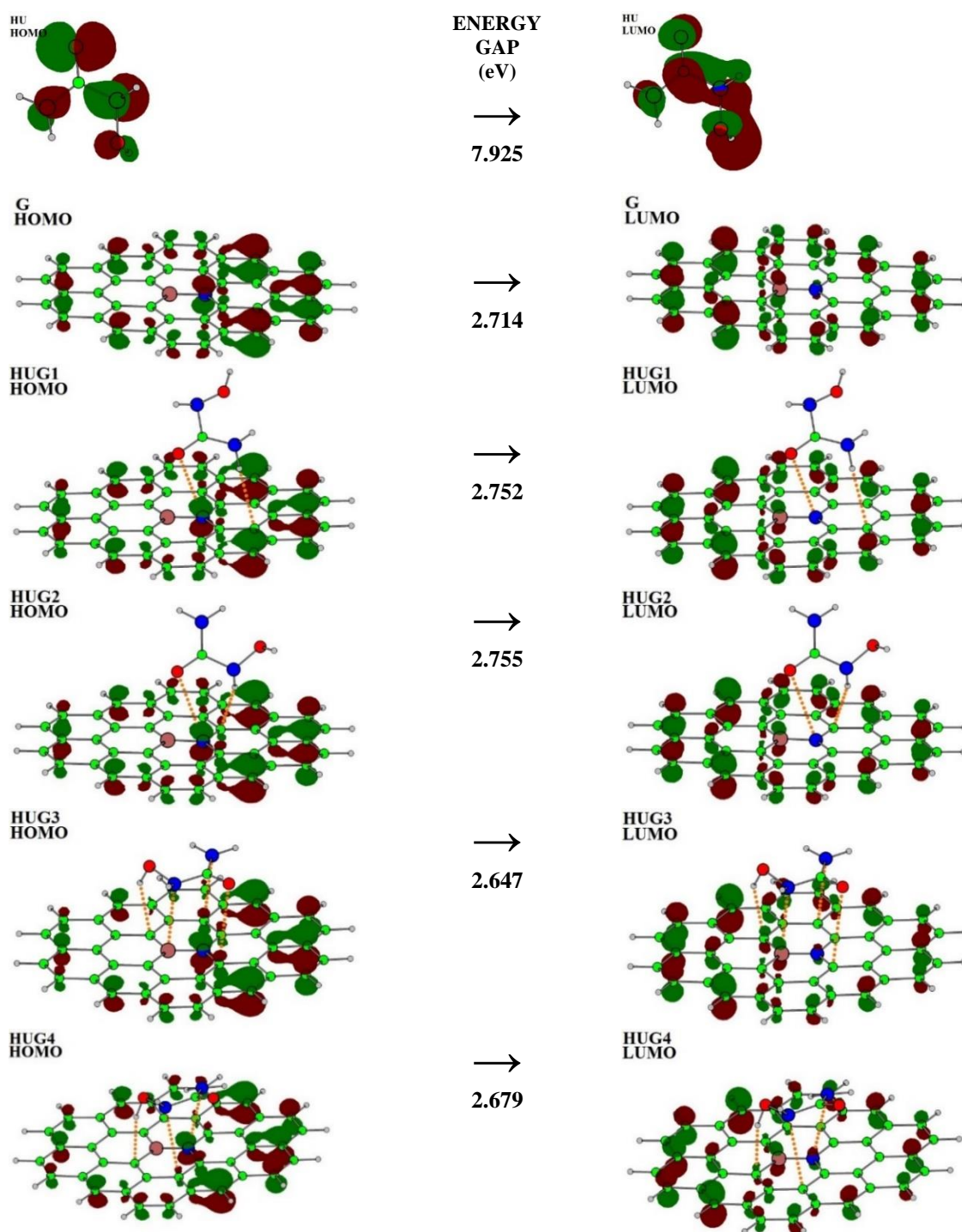


Figure 2. Distribution patterns of HOMO-LUMO for the optimized structures of single and bimolecule models. The energy gap means the energy difference between HOMO and LUMO levels.

Additionally, those features of biomolecules were also seen to be different among the four models of HUG1, HUG2, HUG3, and HUG4. These achievements are very important regarding the role of such energy differences in managing a diagnosis system, as could be seen by the values of EG as the energy gap between HOMO and LUMO levels, the models detectable upon measuring such EG features. The single HU and the single G were in different HOMO, LUMO, and EG levels, compared with the bimolecule state models. As a consequence, formations of HUG complexes could be detectable in accordance with such molecular orbitals

energy features. Additionally, different levels of HOMO and LUMO for the models of a single state could make it possible to occur an interaction between them. Next, the models were found with significant changes in such states.

The obtained values of EG were 7.925 eV and 2.714 eV for the single HU and G models, in which they were changed into 2.752 eV, 2.755 eV, 2.647 eV, and 2.679 eV, in each of HUG1, HUG2, HUG3, and HUG4 biomolecule models. Interestingly, an order of HUG3 < HUG4 < HUG1 < HUG2 was found for the EG values of biomolecules in a reversed direction of the obtained values of ADS. In this regard, a model with a higher level of adsorption strength could show a closer distance between HOMO and LUMO levels. Further analyses of the related features to the energy of the molecular orbitals were based on chemical hardness (CH), chemical potential (CP), and electrophilicity index (EI), in which they all showed variations of electronic features for the investigated biomolecules. Indeed, these electronic-based features are very important for specifying a function to the models for working in the desired route. For visualizing localizations of HOMO and LUMO levels, distribution patterns for the optimized single and biomolecule were exhibited in Figure 2.

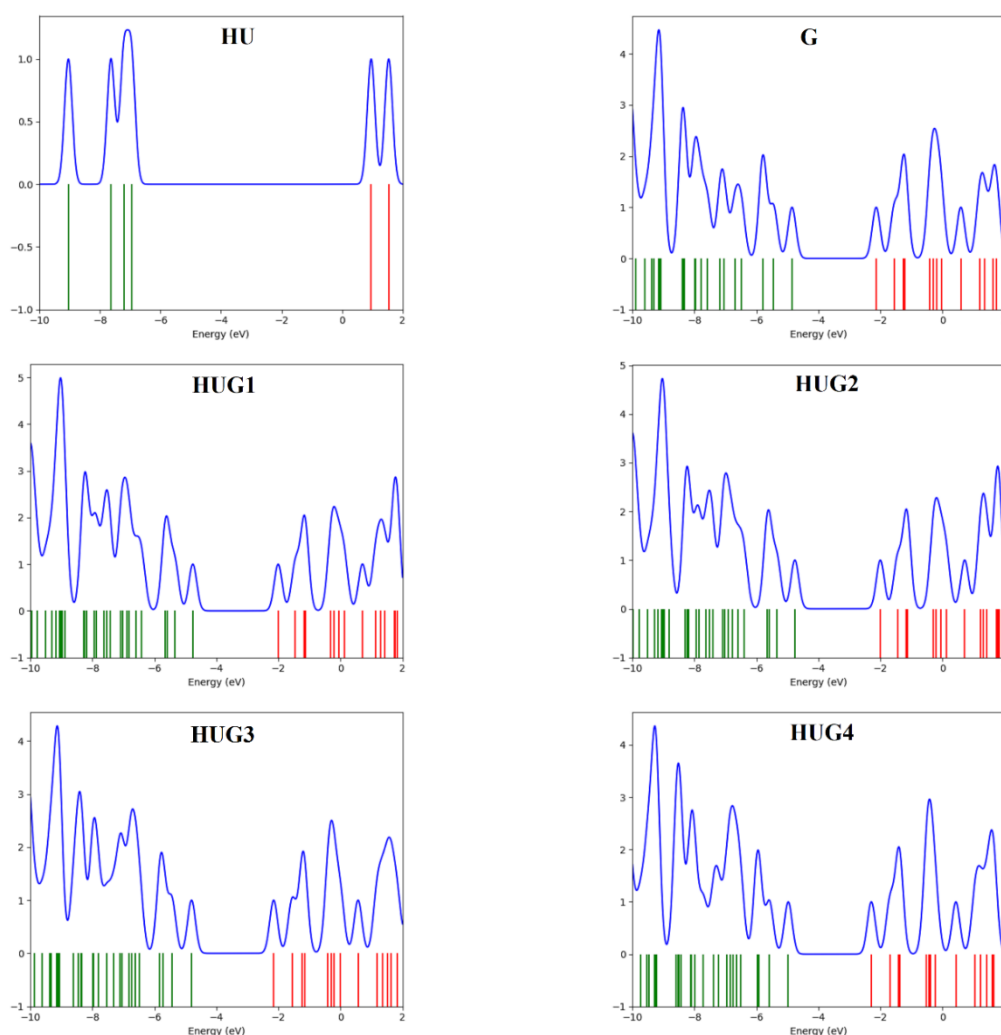


Figure 3. DOS diagrams for the optimized structures of single and biomolecule models. Green, red, and blue colors show occupied orbitals, unoccupied orbitals, and DOS diagrams.

For showing variations of molecular orbitals before and after each of the HOMO and LUMO levels, the illustrated diagrams of DOS (Figure 3) could help to see such variations among the models. Indeed, the diagrams could show the route of measurement of electronic molecular orbitals variations for approaching a diagnosis level of employing the G surfaces <https://biointerfaceresearch.com/>

towards the HU substance. From single state to bimolecule state, distribution of both HOMO and LUMO levels were concentrated on the G substance of HUG bimolecule models making the adsorbed HU substance free of any molecular orbitals localizations. This achievement could refer to a dominant role of the G surface for the successful adsorption of HU substance to create HUG bimolecules. Next, the G adsorbent could protect the adsorbed HU not to participate in further reactions or interactions unless the equivalent desorption energy is provided. This is important for conducting a targeted drug delivery platform for carrying the drug to the specific target. In this regard, the results indicated that the adsorption process of HU substance at the G surface could be achievable with the possibility of measuring variations of molecular orbitals features to approach a diagnosis point. As a consequence, the obtained results almost affirmed the initial hypothesis of this work for assessing the G surface for the drug delivery of HU anticancer.

4. Conclusions

This work could be summarized in accordance with its major goal to assess a BN-doped graphene (G) model for the drug delivery of hydroxyurea (HU) anticancer. The results indicated a meaningful formation of HUG biomolecules through the occurred interactions of HU and G substances. The BN-doped region of the surface helped to manage the interaction processes. Details of interactions showed a reasonable physical strength of HUG formation for keeping the HU substance at the G surface. Additionally, details of QTAIM analyses indicated the existence of physical interactions for forming HUG complexes. Four bimolecule models, including HUG1, HUG2, HUG3, and HUG4, were found based on the relaxation of HU towards the G surface, in which their strength and electronic features were different. Moreover, the results of molecular orbitals energy indicated the possibility of approaching a diagnosis system for affirming the adsorption of HU at the G surface besides detecting the relaxed configuration. A protective role of G for preventing the adsorbed HU substance not to interact/reacting with other substances was also observed regarding the importance of conducting targeted drug delivery processes. Consequently, this work's results showed the possibility of employing the investigated G model for conducting the drug delivery platform of HU anticancer.

Funding

This research received no external funding.

Acknowledgments

This research has no acknowledgment.

Conflicts of Interest

The authors declare no conflict of interest.

References

1. Kumar, N.; Salehiyan, R.; Chauke, V.; Botlhoko, O.J.; Setshedi, K.; Scriba, M.; Masukume, M.; Ray, S.S. Top-down synthesis of graphene: a comprehensive review. *FlatChem* **2021**, *27*, 100224, <https://doi.org/10.1016/j.flatc.2021.100224>.

2. Farhadi, B.; Ebrahimi, M.; Morsali, A. Pre-concentration and sensitive determination of propranolol and metoprolol using dispersive solid-phase microextraction and high-performance liquid chromatography in biological, wastewater, and pharmaceutical samples. *Chemical Methodologies* **2022**, *6*, 750-761, <https://doi.org/10.22034/chemm.2022.317197.1401>.
3. Kumar, V.; Kumar, A.; Lee, D.J.; Park, S.S. Estimation of number of graphene layers using different methods: a focused review. *Materials* **2021**, *14*, 4590, <https://doi.org/10.3390/ma14164590>.
4. Pour Karim, S.; Ahmadi, R.; Yousefi, M.; Kalateh, K.; Zarei, G. Interaction of graphene with amoxicillin antibiotic by in silico study. *Chemical Methodologies* **2022**, *6*, 861-871, <https://doi.org/10.22034/chemm.2022.347571.1560>.
5. Abu-Nada, A.; Abdala, A.; McKay, G. Removal of phenols and dyes from aqueous solutions using graphene and graphene composite adsorption: a review. *Journal of Environmental Chemical Engineering* **2021**, *9*, 105858, <https://doi.org/10.1016/j.jece.2021.105858>.
6. Hamidi Zare, S.; Ghorayshi Nejad, M.; Saberi, A.; Rostami, E. A highly efficient and sustainable synthesis of 1-[(1,3-thiazol-2-ylamino) methyl]-2-naphthols under solvent-free conditions using graphene oxide substituted ethane sulfonic acid catalyst. *Asian Journal of Nanosciences and Materials* **2022**, *5*, 211-224, http://www.ajnanomat.com/article_155115.html.
7. Hedayatipannah, M.; Gholami, L.; Farhadian, M.; Purjebreil, M.; Farmany, A. Medical and chemical evaluation of the effectiveness of the new spray in preventing the formation of dental plaque. *Journal of Medicinal and Chemical Sciences* **2022**, *5*, 637-646, <https://doi.org/10.26655/JMCHEMSCI.2022.4.20>.
8. Kong, Q.; Shi, X.; Ma, W.; Zhang, F.; Yu, T.; Zhao, F.; Zhao, D.; Wei, C. Strategies to improve the adsorption properties of graphene-based adsorbent towards heavy metal ions and their compound pollutants: a review. *Journal of Hazardous Materials* **2021**, *415*, 125690, <https://doi.org/10.1016/j.jhazmat.2021.125690>.
9. Ali Fadhil, H.; H. Samir, A.; Abdulghafoor Mohammed, Y.; M.M. Al. Rubaei, Z. Synthesis, characterization, and in vitro study of novel modified reduced graphene oxide (RGO) containing heterocyclic compounds as anti-breast cancer. *Eurasian Chemical Communications* **2022**, *4*, 1156-1170, <https://doi.org/10.22034/ecc.2022.345188.1484>.
10. Kamel Attar Kar, M.H.; Yousefi, M. Investigating drug delivery of 5-fluorouracil by assistance of an iron-modified graphene scaffold: computational studies. *Main Group Chemistry* **2022**, *21*, 651-658, <https://doi.org/10.3233/MGC-210164>.
11. Tallapaneni, V.; Mude, L.; Pamu, D.; Karri, V. Formulation, characterization and in vitro evaluation of dual-drug loaded biomimetic chitosan-collagen hybrid nanocomposite scaffolds. *Journal of Medicinal and Chemical Sciences* **2022**, *5*, 1059-1074, <https://doi.org/10.26655/JMCHEMSCI.2022.6.19>.
12. Ukwubile, C.; Ikpefan, E.; Otalu, O.; Njidda, S.; Angyu, A.; Menkiti, N. Nanoencapsulation of phthalate from melastomastrum capitatum (Fern.) in chitosan-nps as a target mediated drug delivery for multi-drug resistant pathogen. *International Journal of Advanced Biological and Biomedical Research* **2021**, *9*, 160-180, <https://doi.org/10.22034/ijabbr.2021.241725>.
13. Baghernejad, B.; Hojjati Taromsari, S. Aqueous media preparation of 2-amino-4H-benzopyran derivatives using cerium oxide nanoparticles as a recyclable catalyst. *Asian Journal of Green Chemistry* **2022**, *6*, 194-202, <https://doi.org/10.22034/ajgc.2022.3.2>.
14. Ozkendir, O.M.; Cengiz, E.; Mirzaei, M.; Karahan, I.H.; Özdemir, R.; Klysubun, W. Electronic structure study of the bimetallic Cu_{1-x}Zn_x alloy thin films. *Materials Technology* **2018**, *33*, 193-197, <https://doi.org/10.1080/10667857.2017.1391932>.
15. Mortezagholi, B.; Movahed, E.; Fathi, A.; Soleimani, M.; Forutan Mirhosseini, A.; Zeini, N.; Khatami, M.; Naderifar, M.; Abedi Kiasari, B.; Zareanshahraki, M. Plant-mediated synthesis of silver-doped zinc oxide nanoparticles and evaluation of their antimicrobial activity against bacteria cause tooth decay. *Microscopy Research and Technique* **2022**, *85*, 3553-3564, <https://doi.org/10.1002/jemt.24207>.
16. Mahmood, S.; Atiya, A.; Abdulrazzak, F.; Alkaim, A.; Hussein, F. A review on applications of carbon nanotubes (CNTs) in solar cells. *Journal of Medicinal and Chemical Sciences* **2021**, *4*, 225-229, <https://doi.org/10.26655/JMCHEMSCI.2021.3.2>.
17. Jassim, L.; Mahmood, K. Study of some physicochemical, microbial and sensory properties of low-fat butter produced by titanium dioxide (TiO₂) nano particles. *Eurasian Chemical Communications* **2022**, *4*, 241-255, <https://doi.org/10.22034/ecc.2022.318882.1275>.
18. Aminian A, Fathi A, Gerami MH, Arsan M, Forutan Mirhosseini A, Torabizadeh SA. Nanoparticles to overcome bacterial resistance in orthopedic and dental implants. *Nanomedicine Research Journal*. 2022 Apr 1;7(2):107-23. http://www.nanomedicine-rj.com/article_253215.html.

19. Alijani, H.Q.; Fathi, A.; Amin, H.I.; Lima Nobre, M.A.; Akbarizadeh, M.R.; Khatami, M.; Jalil, A.T.; Naderifar, M.; Safarpour Dehkordi, F.; Shafiee, A. Biosynthesis of core-shell α -Fe₂O₃@ Au nanotruffles and their biomedical applications. *Biomass Conversion and Biorefinery* **2022**, *in press*, <https://doi.org/10.1007/s13399-022-03561-3>.
20. Mirzaei, M.; Kalhor, H.R.; Hadipour, N.L. Covalent hybridization of CNT by thymine and uracil: a computational study. *Journal of Molecular Modeling* **2011**, *17*, 695-699, <https://doi.org/10.1007/s00894-010-0771-z>.
21. Fathpour, K.; Ahmadabadi, M.N.; Atash, R.; Fathi, A. Effect of different surface treatment methods on the shear bond strength of resin composite/zirconia for intra-oral repair of zirconia restorations. *European Journal of Dentistry* **2022**, *in press*, <http://doi.org/10.1055/s-0042-1756475>.
22. Dehno Khalaji, A.; Macheck, P.; Jarosova, M. α -Fe₂O₃ nanoparticles, synthesis, characterization, magnetic properties and photocatalytic degradation of methyl orange. *Advanced Journal of Chemistry-Section A* **2021**, *4*, 317-326, <https://doi.org/10.22034/ajca.2021.292396.1268>.
23. Ebadian, B.; Fathi, A.; Beiranvand, N. Investigation of the effect of bonding factors on strength of porcelain bond to soft metal alloys after application of thermal cycle. *Dental Research Journal* **2022**, *19*, 91, <http://doi.org/10.4103/1735-3327.359328>.
24. Saliminasab, M.; Jabbari, H.; Farahmand, H.; Asadi, M.; Soleimani, M.; Fathi, A. Study of antibacterial performance of synthesized silver nanoparticles on Streptococcus mutans bacteria. *Nanomedicine Research Journal* **2022**, *7*, 391-396, http://www.nanomedicine-rj.com/article_696643.html.
25. Hameed, S.; Turkie, D. A novel approach for study of surface morphology & roughness analysis for characterization of precipitation product at a nanoscale level via the reaction of fluconazole with phosphomolybdic acid. *Chemical Methodologies* **2022**, *6*, 385-397, <https://doi.org/10.22034/chemm.2022.332594.1450>.
26. Talavari, A.; Ghanavati, B.; Azimi, A.; Sayyahi, S. PVDF/ MWCNT hollow fiber mixed matrix membranes for gas absorption by Al₂O₃ nanofluid. *Progress in Chemical and Biochemical Research* **2021**, *4*, 177-190, <https://doi.org/10.22034/pabr.2021.270178.1177>.
27. Jasim, D.; Abbas, A. Synthesis, identification, antibacterial, medical and dyeing performance studies for azo-sulfamethoxazole metal complexes. *Eurasian Chemical Communications* **2022**, *4*, 16-40, <https://doi.org/10.22034/ecc.2022.310593.1251>.
28. Ghalehassadi, M.; Ziaei, M.; Rezaei, E. Synthesis of some silyl derivatives of graphene oxide. *Main Group Chemistry* **2021**, *20*, 119-132, <https://doi.org/10.3233/MGC-201217>.
29. Oji Moghanlou, A.; Salimi, F. The investigation of antibacterial activity and cell viability of rGO/Cu₂O nanocomposite. *Asian Journal of Nanosciences and Materials* **2022**, *5*, 63-78, <https://doi.org/10.26655/ajnanomat.2022.1.6>.
30. Wikantyasning, E.R.; Kalsum, U.; Nurfiani, S.; Da'i, M.; Choliso, Z. Allylamine-conjugated polyacrylic acid and gold nanoparticles for colorimetric detection of bacteria. *Materials Science Forum* **2021**, *1029*, 137-144, <https://doi.org/10.4028/www.scientific.net/MSF.1029.137>.
31. Tosan, F.; Rahnama, N.; Sakhaei, D.; Fathi, A.; Yari, A. Effects of doping metal nanoparticles in hydroxyapatite in Improving the physical and chemical properties of dental implants. *Nanomedicine Research Journal* **2021**, *6*, 327-336, http://www.nanomedicine-rj.com/article_249480.html.
32. Sheikholeslami-Farahani, F. Amine functionalized SiO₂@Fe₃O₄ as a green and reusable magnetic nanoparticles system for the synthesis of Knoevenagel condensation in water. *Asian Journal of Nanosciences and Materials* **2022**, *5*, 132-143, <https://doi.org/10.26655/ajnanomat.2022.2.5>.
33. Bie, C.; Yu, H.; Cheng, B.; Ho, W.; Fan, J.; Yu, J. Design, fabrication, and mechanism of nitrogen-doped graphene-based photocatalyst. *Advanced Materials* **2021**, *33*, 2003521, <https://doi.org/10.1002/adma.202003521>.
34. Dessie, Y., Tadesse, S. A review on advancements of nanocomposites as efficient anode modifier catalyst for microbial fuel cell performance improvement. *Journal of Chemical Reviews* **2021**, *3*, 320-344, <https://doi.org/10.22034/jcr.2021.314327.1128>.
35. Baghernejad, B., Alikhani, M. Nano-Cerium Oxide/Aluminum Oxide as an Efficient Catalyst for the Synthesis of Xanthene Derivatives as Potential Antiviral and Anti-Inflammatory Agents. *Journal of Applied Organometallic Chemistry* **2022**, *2*, 155-162, <https://doi.org/10.22034/jaoc.2022.154819>.
36. Hoseini, Z.; Davoodnia, A.; Pordel, M. Another successful application of newly prepared GO-SiC₃-NH₃-H₂PW as highly efficient nanocatalyst for fast synthesis of tetrahydrobenzo[b]pyrans. *Advanced Journal of Chemistry-Section A* **2021**, *4*, 68-77, <https://doi.org/10.22034/ajca.2021.259593.1228>.

37. Sukmawati, A.; Utami, W.; Yuliani, R.; Da'i, M.; Nafarin, A. Effect of tween 80 on nanoparticle preparation of modified chitosan for targeted delivery of combination doxorubicin and curcumin analogue. *IOP Conference Series: Materials Science and Engineering* **2018**, *311*, 012024, <https://doi.org/10.1088/1757-899X/311/1/012024>.
38. Farhami, N. A computational study of thiophene adsorption on boron nitride nanotube. *Journal of Applied Organometallic Chemistry* **2022**, *2*, 163-172, <https://doi.org/10.22034/jaoc.2022.154821>.
39. Golipour-Chobar, E.; Salimi, F.; Ebrahimzadeh-Rajaei, G. Sensing of lomustine drug by pure and doped C48 nanoclusters: DFT calculations. *Chemical Methodologies* **2022**, *6*, 790-800, <https://doi.org/10.22034/chemm.2022.344895.1555>.
40. Jalali Sarvestani, M. The effect of doping graphene with silicon on the adsorption of cadmium(II), theoretical investigations. *Asian Journal of Nanosciences and Materials* **1999**, *3*, 280-290, <https://doi.org/10.26655/ajnanomat.2020.4.2>.
41. Ghanavati, B.; Bozorgian, A.; Kazemi Esfeh, H. Thermodynamic and kinetic study of adsorption of cobalt II using adsorbent of magnesium oxide nano-particles deposited on chitosan. *Progress in Chemical and Biochemical Research* **2022**, *5*, 165-181, <https://doi.org/10.22034/pcbr.2022.335475.1219>.
42. Hatami, A.; Heydarinasab, A.; Akbarzadehkhayavi, A.; Pajoum Shariati, F. An introduction to nanotechnology and drug delivery. *Chemical Methodologies* **2021**, *5*, 153-165, <https://doi.org/10.22034/chemm.2021.121496>.
43. Shahamatpour, M.; Tabatabaee Ghomsheh, S.; Maghsoudi, S.; Azizi, S. Fenton processes, adsorption and nano filtration in industrial wastewater treatment. *Progress in Chemical and Biochemical Research* **2021**, *4*, 32-43, <https://doi.org/10.22034/pcbr.2021.118152>.
44. Dhahir, Z.; Turkie, N. New turbidimetric method for determination of cefotaxime sodium in pharmaceutical drugs using continuous flow injection manifold design with CFTS-vanadium oxide sulfate system. *Chemical Methodologies* **2022**, *6*, 91-102, <https://doi.org/10.22034/chemm.2022.2.2>.
45. Ishii, T.; Philavanh, M.; Negishi, J.; Inukai, E.; Ozaki, J.I. Preparation of chemically structure-controlled BN-doped carbons for the molecular understanding of their surface active sites for oxygen reduction reaction. *ACS Catalysis* **2022**, *12*, 1288-1297, <https://doi.org/10.1021/acscatal.1c04806>.
46. Darougari, H.; Rezaei-Sameti, M. The drug delivery appraisal of Cu and Ni decorated B12N12 nanocage for an 8-hydroxyquinoline drug: a DFT and TD-DFT computational study. *Asian Journal of Nanosciences and Materials* **2022**, *5*, 196-210, http://www.ajnanomat.com/article_154625.html.
47. Anafcheh, M. A comparison between density functional theory calculations and the additive schemes of polarizabilities of the Li-F-decorated BN cages. *Journal of Applied Organometallic Chemistry* **2021**, *1*, 125-133, <https://doi.org/10.22034/jaoc.2021.292384.1027>.
48. Herrera-Reinoza, N.; dos Santos, A.C.; de Lima, L.H.; Landers, R.; de Siervo, A. Atomically precise bottom-up synthesis of h-BNC: graphene doped with h-BN nanoclusters. *Chemistry of Materials* **2021**, *33*, 2871-2882, <https://doi.org/10.1021/acs.chemmater.1c00081>.
49. Islami, F.; Guerra, C.E.; Minihan, A.; Yabroff, K.R.; Fedewa, S.A.; Sloan, K.; Wiedt, T.L.; Thomson, B.; Siegel, R.L.; Nargis, N.; Winn, R.A. American Cancer Society's report on the status of cancer disparities in the United States, 2021. *CA: A Cancer Journal for Clinicians* **2022**, *72*, 112-143, <https://doi.org/10.3322/caac.21703>.
50. Hatami, A. Preparation, description and evaluation of the lethality acid loaded liposomal nanoparticles against in vitro colon and liver cancer. *Journal of Chemical Reviews* **2021**, *3*, 121-133, <https://doi.org/10.22034/jcr.2021.283609.1109>.
51. Ali Salman, R. Immunohistochemical determination of estrogen and progesterone receptors in women breast cancer patients. *Journal of Medicinal and Chemical Sciences* **2022**, *5*, 1224-1230, <https://doi.org/10.26655/JMCS.2022.7.11>.
52. Maghsoudi, S.; Hosseini, S.; Ravandi, S. A review on phospholipid and liposome carriers: synthetic methods and their applications in drug delivery. *Journal of Chemical Reviews* **2022**, *4*, 346-363, <https://doi.org/10.22034/jcr.2022.355104.1182>.
53. Matthews, H.K.; Bertoli, C.; de Bruin, R.A. Cell cycle control in cancer. *Nature Reviews Molecular Cell Biology* **2022**, *23*, 74-88, <https://doi.org/10.1038/s41580-021-00404-3>.
54. Bashiri Godarzi, F.; Shamaei, S. Evaluation of anti-bacterial (*Escherichia coli* and *Staphylococcus aureus*) and anticancer effects of silver nanoparticles synthesized by *Melissa officinalis* L. extract on several cancer cells (A549, MCF-7, and HeLa). *International Journal of Advanced Biological and Biomedical Research* **2022**, *10*, 57-71, <https://doi.org/10.22034/ijabbr.2022.548282.1380>.

55. Waheed, S.; Mustafa, Y. Synthesis and evaluation of new coumarins as antitumor and antioxidant Applicants. *Journal of Medicinal and Chemical Sciences* **2022**, *5*, 808-819, <https://doi.org/10.26655/JMCHEMSCI.2022.5.15>.
56. Hakimian, H.; Rezaei-Zarchi, S.; Javid, A. The toxicological effect of *Cuscuta epithymum* and *Artemisia absinthium* species on CP70 ovarian cancer cells. *International Journal of Advanced Biological and Biomedical Research* **2021**, *9*, 331-339, <https://doi.org/10.22034/ijabbr.2021.526486.1355>.
57. Abyar Ghamsari, P.; Samadzadeh, M. 4-Amino modified derivatives of cytidine towards interactions with the methyltransferase enzyme. *Main Group Chemistry* **2022**, *21*, 903-917, <https://doi.org/10.3233/MGC-210185>.
58. Ghanadian, M.; Ali, Z.; Khan, I.A.; Balachandran, P.; Nikahd, M.; Aghaei, M.; Mirzaei, M.; Sajjadi, S.E. A new sesquiterpenoid from the shoots of Iranian *Daphne mucronata* Royle with selective inhibition of STAT3 and Smad3/4 cancer-related signaling pathways. *DARU Journal of Pharmaceutical Sciences* **2020**, *28*, 253-262, <https://doi.org/10.1007/s40199-020-00336-x>.
59. Hammoodi, S.; Ismael, S.; Mustafa, Y. Mutual prodrugs for colon targeting: a review. *Eurasian Chemical Communications* **2022**, *4*, 1251-1265, <https://doi.org/10.22034/ecc.2022.351682.1506>.
60. Hantoush, A.; Najim, Z.; Abachi, F. Density functional theory, ADME and docking studies of some tetrahydropyrimidine-5- carboxylate derivatives. *Eurasian Chemical Communications* **2022**, *4*, 778-789, <https://doi.org/10.22034/ecc.2022.333898.1374>.
61. Hudiawati, D.; Syafitry, W. Effectiveness of physical and psychological treatment for cancer-related fatigue: systematic review. *Jurnal Kesehatan* **2021**, *14*, 195, <https://doi.org/10.23917/jk.v14i2.15596>.
62. Saroyo, H.; Saputri, N.F. Cytotoxicity of mangrove leaves (*rhizophora*) ethanolic extract on cancer cells. *Journal of Nutraceuticals and Herbal Medicine* **2021**, *4*, 43, <https://doi.org/10.23917/jnhm.v4i1.15657>.
63. Khosravian, M.; Momenzadeh, M.; Koosha, F.; Alimohammadi, N.; Kianpour, N. Lung cancer risk and the inhibitors of angiotensin converting enzyme; an updated review on recent evidence. *Immunopathologia Persa* **2022**, *8*, e19, <https://doi.org/10.34172/ipp.2022.19>.
64. Asgharpour, M.; Kalan, M.E.; Mirhashemi, S.H.; Alirezaei, A. Lung cancer risk and the inhibitors of angiotensin converting enzyme: a mini-review of recent evidence. *Immunopathologia Persa* **2019**, *5*, e16, <https://doi.org/10.15171/ipp.2019.16>.
65. Mohammed, B.G. Identification of genetic markers of drug resistance and virulence factor gene in *campylobacter jejuni* isolated from children in north Iraq. *Journal of Medicinal and Chemical Sciences* **2022**, *5*, 1191-1199, <https://doi.org/10.26655/JMCHEMSCI.2022.7.7>.
66. Hiawi, F.A.; Ali, I.H. Study the adsorption behavior of food colorant dye indigo carmine and loratadine drug in solution. *Chemical Methodologies* **2022**, *6*, 720-730, <https://doi.org/10.22034/chemm.2022.349806.1570>.
67. Fathi, A.; Rismanchian, M.; Dezaki, S.N. Effectiveness of different antimicrobial agents on malodor prevention in two-stage dental implants: a double-blinded randomized clinical trial. *European Journal of Dentistry* **2022**, *in press*, <https://doi.org/doi.org/10.1055/s-0042-1747954>.
68. Khamisi, N.; Fathi, A.; Yari, A. Antimicrobial resistance of *Staphylococcus aureus* isolated from dental plaques. *Academic Journal of Health Sciences: Medicina Balear* **2022**, *37*, 136-140, <https://doi.org/10.3306/AJHS.2022.37.01.136>.
69. Rankine-Mullings, A.E.; Nevitt, S.J. Hydroxyurea (hydroxycarbamide) for sickle cell disease. *Cochrane Database of Systematic Reviews* **2022**, <https://doi.org/10.1002/14651858.CD002202.pub3>.
70. Yasara, N.; Wickramaratne, N.; Mettananda, C.; Silva, I.; Hameed, N.; Attanayaka, K.; Rodrigo, R.; Wickramasinghe, N.; Perera, L.; Manamperi, A.; Premawardhena, A. A randomised double-blind placebo-controlled clinical trial of oral hydroxyurea for transfusion-dependent β -thalassaemia. *Scientific Reports* **2022**, *12*, 2752, <https://doi.org/10.1038/s41598-022-06774-8>.
71. Rahimi, R.; Solimannejad, M.; Ehsanfar, Z. Potential application of XC3 (X= B, N) nanosheets in drug delivery of hydroxyurea anticancer drug: a comparative DFT study. *Molecular Physics* **2022**, *120*, e2014587, <https://doi.org/10.1080/00268976.2021.2014587>.
72. Ricchi, P.; Meloni, A.; Rigano, P.; Pistoia, L.; Spasiano, A.; Allò, M.; Messina, G.; Quarta, A.; Rosso, R.; Quota, A.; Filosa, A. The use of hydroxyurea in the real life of MIOT network: an observational study. *Expert Opinion on Drug Safety* **2022**, <https://doi.org/10.1080/14740338.2022.2064980>.
73. Allard, P.; Alhaj, N.; Lobitz, S.; Cario, H.; Jarisch, A.; Grosse, R.; Oevermann, L.; Hakimeh, D.; Tagliaferri, L.; Kohne, E.; Kopp-Schneider, A. Genetic modifiers of fetal hemoglobin affect the course of sickle cell disease in patients treated with hydroxyurea. *Haematologica* **2022**, *107*, 1577-1588, <https://doi.org/10.3324/haematol.2021.278952>.

74. Weinstock, L.B.; Brook, J.B.; Molderings, G.J. Efficacy and toxicity of hydroxyurea in mast cell activation syndrome patients refractory to standard medical therapy: retrospective case series. *Naunyn-Schmiedeberg's Archives of Pharmacology* **2022**, <https://doi.org/10.1007/s00210-022-02282-8>.
75. Ben Mofteh, M.; Eswayah, A. Repurposing of hydroxyurea against COVID-19: a promising immunomodulatory role. *ASSAY and Drug Development Technologies* **2022**, *20*, 55-62, <https://doi.org/10.1089/adt.2021.090>.
76. Coache, D.; Friciu, M.; Bernine Marcellin, R.; Bonnemain, L.; Viau, A.; Roullin, V.G.; Forest, J.M.; Leclair, G. Stability evaluation of compounded hydroxyurea 100 mg/mL oral liquids using a novel analytical method involving chemical derivatization. *PLOS ONE* **2022**, *17*, e0270206, <https://doi.org/10.1371/journal.pone.0270206>.
77. Zhou, Y.; Lu, Q. Hydroxyurea protects against diabetic cardiomyopathy by inhibiting inflammation and apoptosis. *Biomedicine & Pharmacotherapy* **2022**, *153*, 113291, <https://doi.org/10.1016/j.biopha.2022.113291>.
78. Creary, S.E.; Beeman, C.; Stanek, J.; King, K.; McGann, P.T.; O'Brien, S.H.; Liem, R.I.; Holl, J.; Badawy, S.M. Impact of hydroxyurea dose and adherence on hematologic outcomes for children with sickle cell anemia. *Pediatric Blood & Cancer* **2022**, *69*, e29607, <https://doi.org/10.1002/pbc.29607>.
79. Gambichler, T.; Stockfleth, E.; Susok, L. Aggressive cutaneous squamous cell carcinoma in a hydroxyurea- and ruxolitinib-pretreated patient with polycythaemia vera. *Journal of the European Academy of Dermatology and Venereology* **2022**, *36*, 63-65, <https://doi.org/10.1111/jdv.17406>.
80. Kantharaj, V.; Ramasamy, N.K.; Yoon, Y.E.; Cheong, M.S.; Kim, Y.N.; Lee, K.A.; Kumar, V.; Choe, H.; Kim, S.Y.; Chohra, H.; Lee, Y.B. Auxin-glucose conjugation protects the rice (*Oryza sativa* L.) seedlings against hydroxyurea-induced phytotoxicity by activating UDP-glucosyltransferase enzyme. *Frontiers in Plant Science* **2022**, *12*, 767044, <https://doi.org/10.3389/fpls.2021.767044>.
81. Dhonnar, S.; Sadgir, N.; Adole, V.; Jagdale, B. Molecular structure, FT-IR spectra, MEP and HOMO-LUMO investigation of 2-(4-fluorophenyl)-5-phenyl-1, 3,4-oxadiazole using DFT theory calculations. *Advanced Journal of Chemistry-Section A* **2021**, *4*, 220-230, <https://doi.org/10.22034/ajca.2021.283003.1254>.
82. Sabe, V.T.; Ntombela, T.; Jhamba, L.A.; Maguire, G.E.; Govender, T.; Naicker, T.; Kruger, H.G. Current trends in computer aided drug design and a highlight of drugs discovered via computational techniques: a review. *European Journal of Medicinal Chemistry* **2021**, *224*, 113705, <https://doi.org/10.1016/j.ejmech.2021.113705>.
83. Ajala, A.; Uzairu, A.; Shallangwa, G.; Abechi, S. In-silico design, molecular docking and pharmacokinetics studies of some tacrine derivatives as anti-alzheimer agents: theoretical investigation. *Advanced Journal of Chemistry-Section A* **2022**, *5*, 59-69, <https://doi.org/10.22034/ajca.2022.321171.1292>.
84. Mirzaei, M.; Hadipour, N.L. An investigation of hydrogen-bonding effects on the nitrogen and hydrogen electric field gradient and chemical shielding tensors in the 9-methyladenine real crystalline structure, a density functional theory study. *The Journal of Physical Chemistry A* **2006**, *110*, 4833-4838, <https://doi.org/10.1021/jp0600920>.
85. Frisch, M.J.; Trucks, G.W.; Schlegel, H.B. et al. Gaussian 09 program. *Gaussian Inc.* **2009**, Wallingford, CT, <https://gaussian.com/g09citation/>.
86. Cortés-Guzmán, F.; Bader, R.F. Complementarity of QTAIM and MO theory in the study of bonding in donor-acceptor complexes. *Coordination Chemistry Reviews* **2005**, *249*, 633-662, <https://doi.org/10.1016/j.ccr.2004.08.022>.
87. Kadhim, M.M.; Sheibanian, N.; Ashoori, D.; Sadri, M.; Tavakoli-Far, B.; Khadivi, R.; Akhavan-Sigari, R. The drug delivery of hydrea anticancer by a nanocone-oxide: Computational assessments. *Computational and Theoretical Chemistry* **2022**, *1215*, 113843, <https://doi.org/10.1016/j.comptc.2022.113843>.
88. Li, W.; Zhao, T. Hydroxyurea anticancer drug adsorption on the pristine and doped C70 fullerene as potential carriers for drug delivery. *Journal of Molecular Liquids* **2021**, *340*, 117226, <https://doi.org/10.1016/j.molliq.2021.117226>.